Combining pressure and particle velocity sensors for seismic processing

P. Felisberto, P. Santos, D. Maslov, S.M. Jesus

LARSyS, University of Algarve

Faro, Portugal

Email: {pfelis, pjsantos, dmaslov, sjesus}@ualg.pt

Abstract—This work discusses the combination of pressure and particle velocity measurements in a single sensing element for underwater seismic applications. In such applications the sensing elements, usually pressure sensors arranged in linear arrays (streamers), receive from the bottom layered structure replicas of a broadband signal generated by a seismic source. In spite of careful setup of sound-receiver geometries, the useful replicas for bottom characterization are contaminated with other replicas, particularly surface reflected ones (ghosts). Since, single pressure sensors are omni-directional it is difficult, if not impossible, to filter out the nuisance replicas at sensor level. However, sensors composed by collocated or closely located pressure and vector field measurements can achieve spatial selectivity. Herein, we analyze the spatial filtering capabilities of various pressure-pressure, particle velocity-particle velocity and pressure-particle velocity combinations in light of seismic applications for narrow band signals. Simulations with the OASES code show that narrow band spatial filtering characteristics of the various combinations can be extended to broadband signals. These results were verified for experimental data acquired by 10 cm apart vector sensors measuring pressure and particle velocity in the 800-1250 Hz band, during the Makai Experiment 2005 sea trial, off Kauai I., Hawaii (USA).

Index Terms—Seismic imaging, Vector sensors, Spatial filtering.

I. INTRODUCTION

For seismic and acoustic surveys of marine environments, the main parameters to be estimated are the number of sediment layers, their compressional speed and their thickness. Marine seismic reflection surveying is performed by a specially equipped vessel which tow cables of hydrophones (known as streamers) that could be up to 8 km long [1]. The streamers are deployed beneath the ocean surface at a constant distance from the vessel. The main purpose is to acquire reflected signals generated by acoustic sources, usually airguns, that are also deployed beneath the ocean surface, between the vessel and the receivers. The source emitted signals reflect in the ocean bottom layers and are received on the streamers. The direct source - receiver signal and spurious reflections on the ocean surface (sometimes termed as ghosts) are undesirable since they interfere with the bottom information rich signal. The noise generated by the tow vessel is another source of interference for the bottom reflected signals. The effect of these interferences significantly attenuated using sensors with spatial filtering capabilities, which can be achieved using vector sensors.

A vector sensor (VS) measure the acoustic pressure and the acoustic particle velocity. Particle velocity components along each of the three axis can be determined either by pressure gradient using two omnidirectional hydrophones (whose distance should be at least ten times smaller than the wavelength) connected as a dipole, or by using accelerometers. Therefore, when an acoustic pressure hydrophone is collocated with the velocity measurement, a VS is able to measure both the acoustic pressure and the three particle velocity components providing an estimate of the full directional acoustic intensity field. The spatial filtering capabilities of VS have become a subject of investigation in 90's [2], [3], [4], [5]. Most of the research involving VS is related to the capabilities of these sensors for direction of arrival (DOA) estimation, where high performance is exhibited over acoustic pressure only (scalar) hydrophones. However, the VS has been also applied in the estimation of other geometric (source range and depth) and environmental parameters [6], or even for geoacoustic inversion [7], [8], [9].

The purpose of WiMUST project [10] is to address seismic geophysical surveying in a setup composed of a ship towing a source and a receiving array carried by Autonomous Underwater Vehicles (AUV). The mobility of AUVs allows for the design of several configurations of receiver arrays that could be along the horizontal or the vertical axis, providing that such configurations can simultaneously cover shallow and deep water along the open ocean area. Bearing in mind this challenge, a VS can be used with several advantages in the WiMUST project scenario since it can be embarked in an AUV with reduction of energy and space requirements. The motivation of using a VS in an AUV and its advantages in the elimination of the direct and surface reflections (ghosts) of the signal will be presented in the next sections.

This paper is organized as follows: Section II analyses the theory related with various combinations of pressure and vertical particle velocity obtained from measurements of a single vector sensor or closely located hydrophones or even more than one vector sensor. Section III presents their directivity patterns. Section IV shows the ability of the various combinations to filter out surface reflections (ghosts) through broad band simulations using OASES code. Section IV presents the experimental results and Section V draws some conclusions.
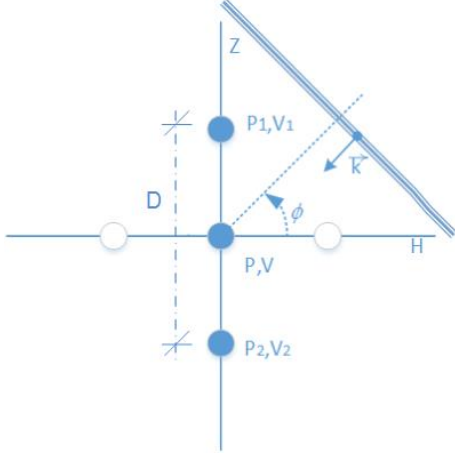
II. THEORETICAL FRAMEWORK

Fig. 1. Geometry definition: the pressure (P_1, P_2) and the (vertical) particle velocity (V_1, V_2) sensors are located along the vertical (Z) axis separated by a distance D. P and V represent the pressure and the (vertical) particle velocity at the origin. The narrow band wavefront is characterized by the wavenumber vector $\vec{k}$ $(k = |\vec{k}| = \omega/c, \omega = 2\pi f$ is the angular frequency, c is the sound speed) and ϕ is the wavefront direction.

A. Particle velocity measurements

The most commonly used methods to measure the particle velocity component along a given axis, is to estimate the pressure gradient using two closely spaced hydrophones or through an accelerometer. This can be carried out either for vertical or horizontal components while hereafter, without loss of generality, we consider the estimation of the vertical (Z) component of the particle velocity. To estimate the particle velocity from the pressure gradient, two pressure sensors P_1 and P_2 aligned with the vertical axis at spacing D are used, Figure 1. The origin is at the middle point between the two pressure sensors and the angle ϕ of the incoming wave is defined relative to the normal of the sensors' axis. When the spacing between pressure sensors D is much smaller than the minimum wavelength λ, the pressure difference can be given by

$$
\begin{aligned}
\frac{P_1(\omega) - P_2(\omega)}{D} &\approx j\frac{\omega}{c}\sin(\phi)P(\omega), \\
&\approx jk\sin(\phi)P(\omega),
\end{aligned}
\tag{1}
$$

where $k = \omega/c$ is the module of the wavenumber vector $\vec{k}$, therefore $k\sin(\phi)$ is the projection of the wavenumber vector onto the sensors' axis.

Thus, the velocity estimate along the (Z) axis, $\hat{V}_z(\omega)$, using the first order differential approximation, is given by

$$
\begin{aligned}
\hat{V}_z(\omega) &= -\frac{1}{j\rho\omega}\frac{P_2(\omega) - P_1(\omega)}{D}\rho c, \\
&= \frac{1}{jk}\frac{P_1(\omega) - P_2(\omega)}{D},
\end{aligned}
\tag{2}
$$

where the scaling factor ρc was applied.

Then, combining Eq. (1) and Eq. (2) allows for obtaining the relation between pressure $P(\omega)$ and the particle velocity $\hat{V}_z(\omega)$ as

$$
\hat{V}_z(\omega) = P(\omega)\sin(\phi).
\tag{3}
$$

When an accelerometer is used, the well known relation between velocity V and acceleration A for a narrow band signal at frequency ω, $A(\omega) = j\omega V(\omega)$, allows to write the pressure equivalent particle velocity as

$$
\hat{V}(\omega) = \frac{\rho}{jk}A(\omega).
\tag{4}
$$

It should be remarked that in both cases the gain (defined as the ratio between the output particle velocity and the pressure or acceleration measurements at a given frequency) is frequency dependent, with a fall of rate of $6\,\text{dB/octave}$ as frequency tends to zero.

B. Combining pressure and particle velocity

One can (linearly) combine the pressure and the particle velocity to obtain $\tilde{P}(\omega)$ as

$$
\tilde{P}(\omega) = P(\omega) + \hat{V}_z(\omega) = P(\omega)(1 + \sin(\phi)),
\tag{5}
$$

using Eq. (3) and where pressure and particle velocity have equal weight in the expression. In case the particle velocity is estimated by two closely located pressure sensors Eq. (2) and the pressure at the middle point between the sensors estimated by averaging, the equation (5) can be written by

$$
\tilde{P}(\omega) = \frac{P_1(\omega) + P_2(\omega)}{2} + \frac{1}{jk}\frac{P_1(\omega) - P_2(\omega)}{D}.
\tag{6}
$$

C. Particle velocity difference

Given two particle velocity measurements $V_1(\omega)$ and $V_2(\omega)$ at close locations (say with a separation D, see Figure 1), one can estimate the (middle point) particle velocity gradient, similar to pressure gradient, as

$$
\bar{V}(\omega) = V(\omega)\sin(\phi) = \frac{1}{jk}\frac{V_1(\omega) - V_2(\omega)}{D},
\tag{7}
$$

where $V(\omega)$ is the particle velocity at the middle point. Equation (7) means that the particle velocity difference is $\bar{V}(\omega) = P(\omega)\sin^2(\phi)$. For close spaced sensors one can write

$$
V_1(\omega) + V_2(\omega) \approx 2V(\omega).
\tag{8}
$$

One defines a linear combination of particle velocity measurements

$$
\tilde{V}(\omega) = \frac{V_1(\omega) + V_2(\omega)}{2} + \frac{1}{jk}\frac{V_1(\omega) - V_2(\omega)}{D},
\tag{9}
$$

therefore

$$
\tilde{V}(\omega) = V(\omega) + V(\omega)\sin(\phi) = P(\omega)(\sin\phi + \sin^2(\phi)).
\tag{10}
$$

III. DIRECTIVITY PATTERN

The spatial filtering characteristics of sensors and sensor arrangements are often described by directivity patterns (or radiation diagrams). Figure 2 compares the normalized directivity patterns (unitary gain at maximum response) for particle velocity (red, Eq. (2)), particle velocity difference only (green, Eq. (7)), a combination of particle velocity and particle velocity difference (black, Eq. (9)) and a combination of pressure and particle velocity (blue, Eq. (6)). In this example,

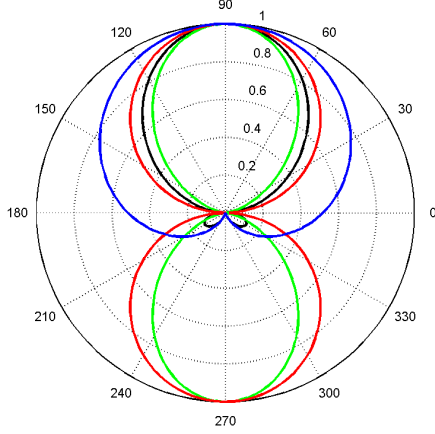Fig. 3. Simulation geometry setup used in the oasp module of OASES.

Fig. 2. Directivity pattern for a pair of sensors placed along the vertical axis (90°): particle velocity (red), particle velocity difference only (green), combination of particle velocity and particle velocity difference (black) and combination of pressure and particle velocity (blue).

the two sensors are aligned with the vertical axis (90°). It can be seen that particle velocity and particle velocity difference only show a "figure of eight"-like directivity pattern, whereas the combination of particle velocity and particle velocity difference or the combination of pressure and particle velocity show a "cardiod"-like directivity. Considering a scenario of geoacoustic survey, a combination of particle velocity sensors aligned with the vertical axis allows to cancel (or significantly attenuate) the direct path and surface reflected paths, usually considered as a nuisance. On the other hand, particle velocity sensors in a horizontal arrangement would cancel the latter arrivals and, when combined with pressure or particle velocity differences, can be used to cancel arrivals from direction opposite to source direction.

IV. SIMULATIONS

The pressure and particle velocity field were computed by the oasp module of OASES [11], [12], using option N for pressure and option V for vertical particle velocity, according to the geometry depicted in Figure 3, which is based on SENSOCEAN'13 experiment setup [13]. The signal is broadband (2000–8000 Hz), with the spectrum shaped by a Hanning window. The particle velocity and the combination of pressure and particle velocity for the frequencies of interest were computed using Eq. (2) and Eq. (6), respectively. Then, the various time domain arrival structures were obtained by inverse Fourier transform.

The echoes at the receiver position are shown in Figure 4 (a) pressure (blue), vertical particle velocity (red, Eq. (2)) and combination of pressure and vertical particle velocity (black, Eq. (6)). The ordering of particle velocity used in the combination of pressure and particle velocity attenuates arrivals impinging the sensor from the sea surface. The various
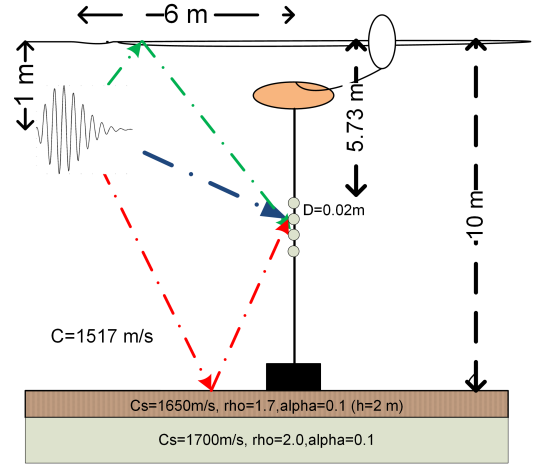
group of echoes of Figure 4 (a) are shown in detail in plots (b) to (e). The first group (Fig. 4 (b)) includes direct and surface reflected echoes, the second group (Fig. 4 (c)) includes the bottom reflected echoes. The third group (Fig. 4 (d)) is composed by the echoes that were surface reflected after a bottom reflection. Finally, the fourth group (Fig. 4 (e)) is composed by the echoes that are reflected from the bottom, after a first bottom reflection followed by a surface-reflection. It can be seen that the combination of pressure and particle velocity is the best suited to filter out direct and surface reflected arrivals. Although, not shown, similar behavior can be obtained using a combination of particle velocity and particle velocity difference as given by Eq. (9).

V. EXPERIMENTAL DATA RESULTS

The data set analyzed herein was acquired during the Makai Experiment (Makai'05), which took place off the west coast of Kauai I. (Hawaii, USA), in September 2005 [14]. This work is concerned with the data acquired during the field calibration event, whose geometry is shown in Figure 5.

The VS acquisition system used in the experiment was composed by four Wilcoxon TV-001 vector sensors [15], configured in a vertical array with 10 cm element spacing. The system was suspended off the stern of the research vessel Kilo Moana, with a 150 kg weight at the bottom, to ensure that the array stayed as close to the vertical as possible. The z-axis was vertically oriented downwards, with the deepest sensor at 40 m. In the present data analysis, the pressure and z-axis (vertical) particle velocity measurements of the two shallowest vector sensors are considered. In the field calibration event, a Lubell 916C sound source deployed at 10 m depth from a small rubber boat was towed during a period of one hour from a 2.5 km distant point towards the research vessel that was holding a fixed position. The signals analyzed herein were acquired when the source-receiver range was approximately 100 m and the water depth was approximately 104 m.
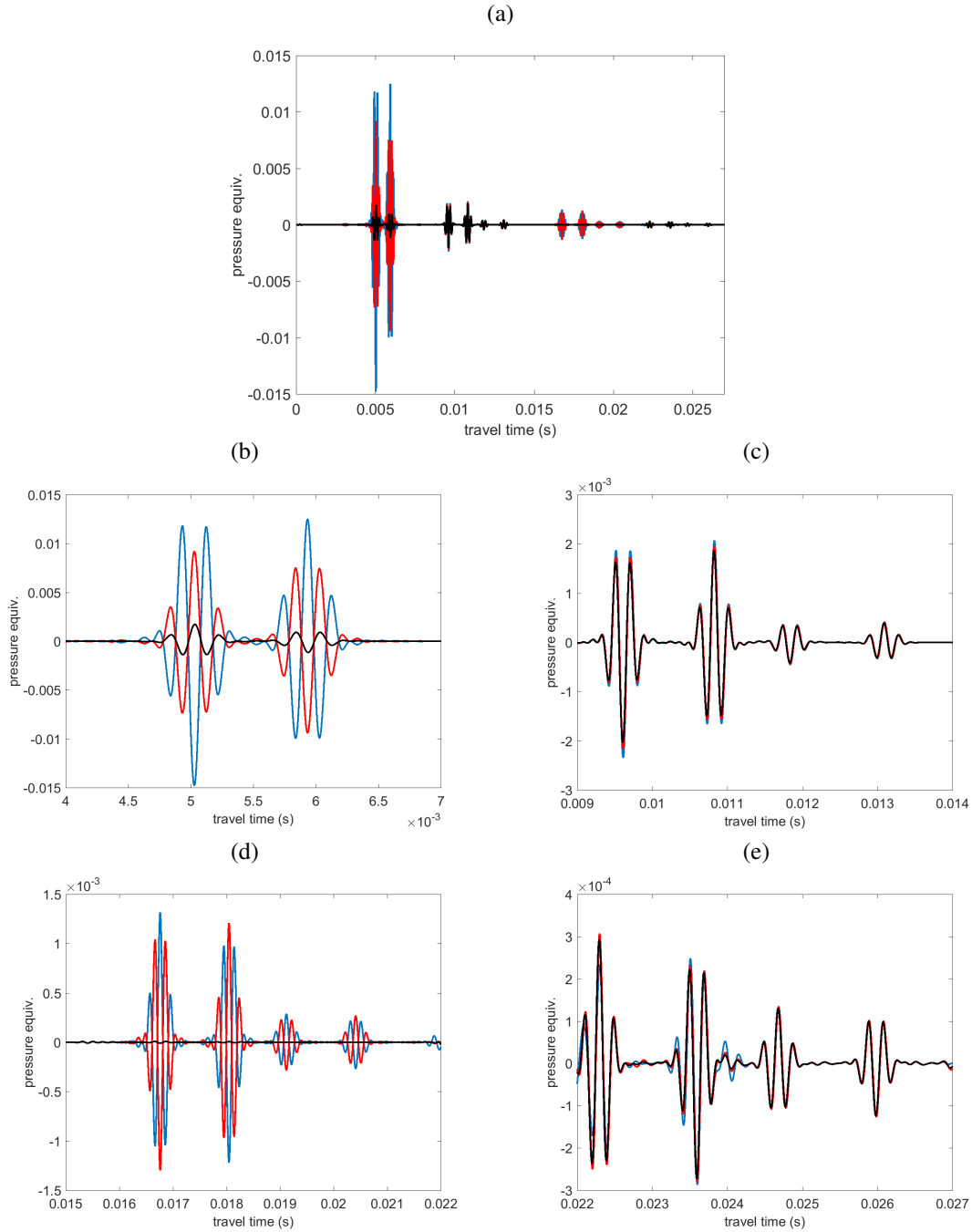
Fig. 4. Signal echoes at receiver position (pressure–blue, vertical particle velocity –red, combination of pressure and vertical particle velocity – black): all arrivals (a) and zoom on direct and surface reflect (b), on bottom reflected (c), on bottom–surface reflected (d) and on bottom-surface–bottom reflected (e).

The Lubell 916C sound source transmitted sequences of LFM chirps, multitones and m-sequences in the 0.5–14 kHz band. The signals were acquired at a sampling frequency of 48 kHz. For the present analysis 4.5 s long LFM chirps spanning the 0.8–1.25 kHz band were used. For further processing, the acquired signals were decimated to 4.8 kHz and filtered in the band 0.5–1.5 kHz by a bandpass linear phase filter to remove the low frequency ship noise and high frequency harmonics of the transmitted signal. Then, the various channels were cross-correlated (match filtered) with the ideal source signal and combined in the frequency domain to obtain the various arrival structures discussed previously. The results are presented in Figure 6 showing the envelopes of the arrival structures. In the upper plots, three group of arrivals can be clearly identified: the first group includes the direct and surface reflected arrivals, the second group includes the bottom reflected arrivals and the third group includes the bottom-surface reflected arrivals.
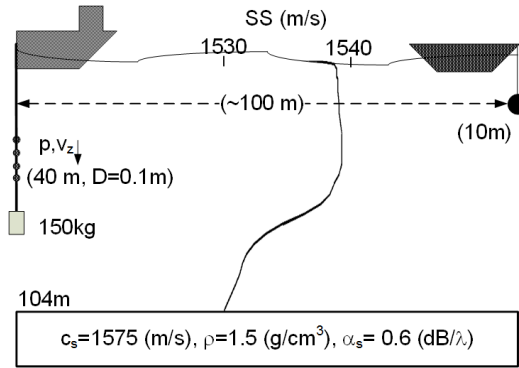
Fig. 5. Makai'05 scenario: the source deployed at 10 m depth is at range about 100 m from the vector sensor deployed with the deepest element at 40 m. The sound speed profile shows a Hawaii characteristic large mixed layer. The bottom parameters are those estimated in [7].

In Figure 6 (a) the blue and green curves were computed from the pressure channel at the two upper vector sensors by the average of the pressure and the combination of the average of the pressure and the pressure gradient, respectively. The red and black curves shown in the same plot were computed from the z-axis particle velocity channels in the same sensors. The red curve represents the vertical particle velocity average, whereas the black curve represents the combination of the vertical particle velocity with the gradient of the vertical particle velocity. The plot in Figure 6 (c) is a zoom of the later arrivals of Figure 6 (a). It can be seen that the combination of pressure or vertical particle velocity with respective gradients either pressure or particle velocity, significantly attenuates the surface arrivals. It should also be noted that the pressure and z-axis particle velocity channels have different gains, what should be accounted for when combining the two data streams (see bellow). Figure 6 (b) shows the arrival structure estimated from a single pressure channel (cyan) with that obtained from the average of two channels (dotted blue) where one can remark their coincidence. The black curve is obtained by a combination of pressure and vertical particle velocity from the measurements of the pressure and z-axis particle velocity channels. For comparison purposes are also included in Figure 6 (b) the green curve (combination of pressure and pressure gradient) and the red curve (z-axis (vertical) particle velocity) of Figure 6 (a). Figure 6 (d) is the zoom of the later arrivals shown in Figure 6 (b). In order to combine the pressure and particle velocity channel the pressure was divided by 3 and the particle velocity was rotated by $\pi/2$ (multiplied by the imaginary unit). The results suggest that using a combination of two VS or even a single VS in a seismic alike geometry allows to filter out undesirable direct and surface-reflected echoes from the received waveforms.

VI. CONCLUSION

The actual seismic streamers are based on linear arrangements of single omni directional hydrophones, which are not able to separate bottom reflections from direct path and surface reflections. The present study suggests that various linear combinations of pressure and/or particle velocity in a single sensing element allow to filter out the undesired signals. The sensing element should, in this case, measure the pressure and the particle velocity by collocated independent sensors, or by at least two pressure or particle velocity sensors (accelerometers) located at a very short distance along the vertical axis. The results show that size and autonomy of such sensor arrangements may advantageously replace short AUV towed streamers for seismic imaging surveys, such as those planned under EU H2020 program funded WiMUST project.

REFERENCES

[1] "Vector sensor applications in underwater acoustics," *https:// en.wikipedia.org/ wiki/ Reflectionseismology*.

[2] A. Nehorai and E. Paldi, "Acoustic vector-sensor array processing," *IEEE Transaction on Signal Processing*, vol. 42, no. 9, pp. 2481–2491, September 1994.

[3] B. Cray and A. Nuttall, "Directivity factors for linear arrays of velocity sensors," *J. Acoust. Soc. Am.*, vol. 110, no. 1, pp. 324–331, July 2001.

[4] C. Wan, A. Kong, and C. Liu, "A comparative study of DOA estimation using vector/gradient sensors," in *Proceedings of Oceans06*, Asia, Pacific, May 16–19 2007, pp. 1–4.

[5] M. Hawkes and A. Nehorai, "Acoustic vector-sensor beamforming and capon direction estimation," *IEEE Trans. Signal Processing*, vol. 46, no. 9, pp. 2291–2304, September 1998.

[6] P. Santos, J. João, O. C. Rodríguez, P. Felisberto, and S. M. Jesus, "Geometric and seabed parameter estimation using a vector sensor array - Experimental results from Makai experiment 2005," in *Proc. MTS/IEEE Oceans'11*, Santander, Spain, June 2011.

[7] P. Santos, O. C. Rodríguez, P. Felisberto, and S. M. Jesus, "Seabed geoacoustic characterization with a vector sensor array," *J. Acoust. Soc. Am.*, vol. 128, no. 5, pp. 2652–2663, November 2010.

[8] H. Peng and F. Li, "Geoacoustic inversion based on a vector hydrophone array," *Chin. Phys. Lett.*, vol. 24, no. 7, pp. 1997–1980, 2007.

[9] P. Santos, *Ocean parameter estimation with High-frequency signals using a Vector Sensor Array*. Faro, Portugal: PhD thesis, University of Algarve, 2012.

[10] H. Al-Khatib, G. Antonelli, A. Caffaz, A. Caiti, G. Casalino, I. B. de Jong, H. Duarte, G. Indiveri, S. Jesus, K. Kebkal, A. Pascoal, and D. Polani, "The widely scalable mobile underwater sonar technology (wimust) project: An overview," in *OCEANS 2015 - Genova*, May 2015, pp. 1–5.

[11] H. Schmidt, "Oases - user guide and reference manual," Department of Ocean Engineering Massachutts Institute of Technology, Tech. Rep. Version 3.1, October 2004.

[12] F. Jensen, W. Kuperman, M. Porter, and H. Schmidt, *Computational Ocean Acoustics*, ser. 2nd Edition. Series in Modern Acoustics and Signal Processing, Springer, NY, 2011.

[13] P. Felisberto, O. C. Rodríguez, P. Santos, F. Zabel, and S. M. Jesus, "Variability of ambient noise over a seagrass bed," in *Proc. MTS/IEEE Oceans'14 Conference*, St. Johns, NL, Canada, September 2014.

[14] M. Porter, B. Abraham, M. Badiey, M. Buckingham, T. Folegot, P. Hursky, S. Jesus, K. Kim, B. Kraft, V. McDonald *et al.*, "The makai experiment: High frequency acoustics," *Proceedings of the 8th ECUA European Conferece on Underwater Acoustic, Carvoeiro, Portugal*, vol. 1215, pp. 918–35, 2006.

[15] J. C. Shipps and B. M. Abraham, "The use of vector sensors for underwater port and waterway security," in *Proceedings of Sensors for Industry conference*, New Orleans, Louisiana, USA, January 2004, pp. 41–44.
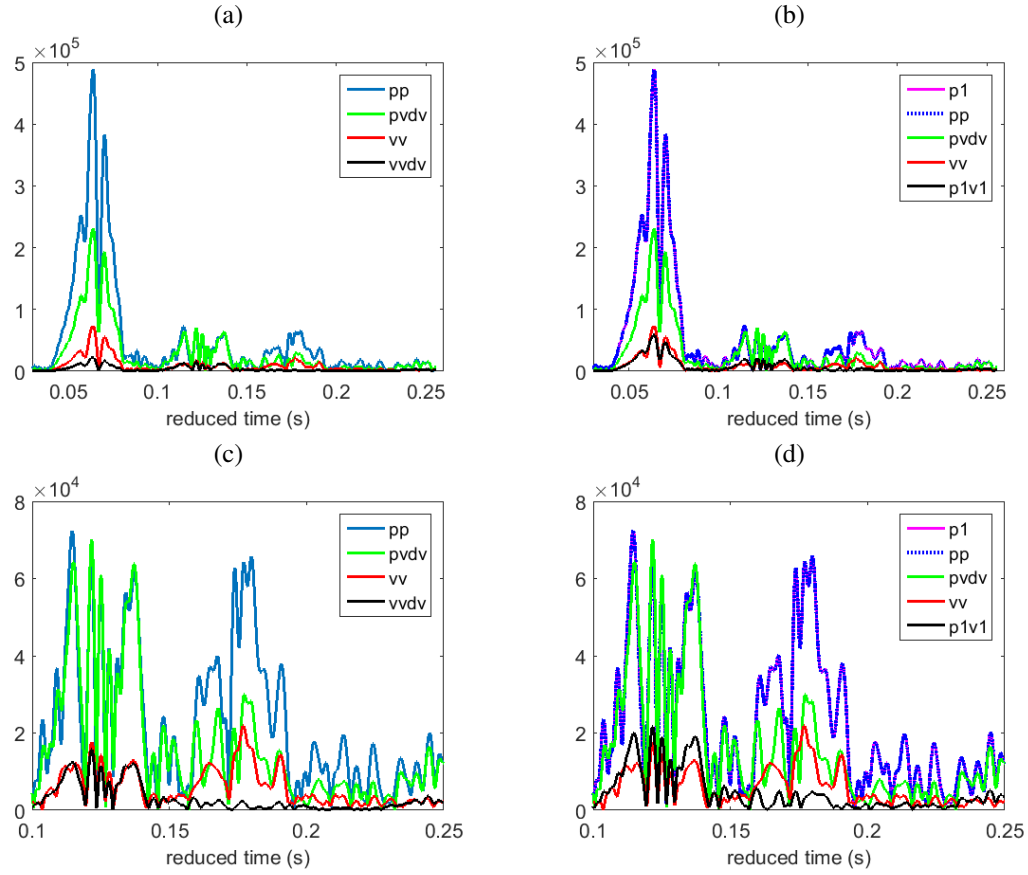
Fig. 6. Arrival patterns computed from waveforms received at minute 56 from run start: (a) pressure (blue), combination of pressure and vertical particle velocity (pressure gradient) estimated from pressure channels (green), particle velocity from z-axis channels (red), combination of particle velocity and particle velocity gradient estimated from z-axis channel (black), (b) pressure from single pressure channel (magenta), pressure from average of pressure channels (dotted blue), combination of pressure and pressure gradient (vertical particle velocity) and vertical estimated from pressure channels (green), particle velocity from z-axis channels (red), combination of pressure and z-axis channels (black), zoom of later arrivals of (a) in (c) and of (b) in (d).